Since January 2020 Elsevier has created a COVID-19 resource centre with free information in English and Mandarin on the novel coronavirus COVID-19. The COVID-19 resource centre is hosted on Elsevier Connect, the company's public news and information website.

Smart Health 25 (2022) 100296

Contents lists available at ScienceDirect

Smart Health

journal homepage: www.elsevier.com/locate/smhl

Convolutional neural network based CT scan classification method for COVID-19 test validation

Mukesh Soni [a,*], Ajay Kumar Singh [b], K. Suresh Babu [c], Sumit Kumar [d], Akhilesh kumar [e], Shweta singh [f]

[a] Department of CSE, University Centre for Research & Development Chandigarh University, Mohali, Punjab, 140413, India
[b] Mody University of Science and Technology, India
[c] Department of Biochemistry, Symbiosis, Medical College for Women, Symbiosis International, Deemed University, Pune, India
[d] Indian Institute of Management, Kozhikode, India
[e] Department of Information Technology, Gaya College, Gaya, Bihar, India
[f] Electronics and Communication Department, IES College of Technology, Bhopal, India

ARTICLE INFO

Keywords:
Novel corona virus
Deep learning
CT image
Conditional generative adversarial network
U-net

ABSTRACT

Given the novel corona virus discovered in Wuhan, China, in December 2019, due to the high false-negative rate of RT-PCR and the time-consuming to obtain the results, research has proved that computed tomography (CT) has become an auxiliary One of the essential means of diagnosis and treatment of new corona virus pneumonia. Since few COVID-19 CT datasets are currently available, it is proposed to use conditional generative adversarial networks to enhance data to obtain CT datasets with more samples to reduce the risk of over fitting. In addition, a BIN residual block-based method is proposed. The improved U-Net network is used for image segmentation and then combined with multi-layer perception for classification prediction. By comparing with network models such as AlexNet and GoogleNet, it is concluded that the proposed BUF-Net network model has the best performance, reaching an accuracy rate of 93%. Using Grad-CAM technology to visualize the system's output can more intuitively illustrate the critical role of CT images in diagnosing COVID-19. Applying deep learning using the proposed techniques suggested by the above study in medical imaging can help radiologists achieve more effective diagnoses that is the main objective of the research. On the basis of the foregoing, this study proposes to employ CGAN technology to augment the restricted data set, integrate the residual block into the U-Net network, and combine multi-layer perception in order to construct new network architecture for COVID-19 detection using CT images. −19. Given the scarcity of COVID-19 CT datasets, it is proposed that conditional generative adversarial networks be used to augment data in order to obtain CT datasets with more samples and therefore lower the danger of overfitting.

1. Introduction

According to Hubei Province's clinical diagnosis criteria, CT scan images are diagnostically significant for COVID-19 severity since

* Corresponding author.
E-mail addresses: mukesh.t1712@cumail.in (M. Soni), ajay.kr.singh07@gmail.com (A.K. Singh), ksuresh.babu@smcw.siu.edu.in (K.S. Babu), sumit01phdpt@iimk.ac.in (S. Kumar), getaky123@gmail.com (A. kumar), pariharshwetasingh90@gmail.com (S. singh).

https://doi.org/10.1016/j.smhl.2022.100296
Received 26 February 2022; Received in revised form 24 April 2022; Accepted 28 May 2022
Available online 11 June 2022

they are incorporated into the definition of pneumonia imaging symptoms. GGO, diffuse alveolar destruction, intraregional vascular thickening, lesions in several lung lobes and the lower pleural area presenting a "crazy-paving" form, etc. are the most conspicuous features of COVID-19 chest CT scans (Jiang et al., 2021). A computer-aided diagnostic system for COVID-19 should be developed in order to quickly identify COVID-19 cases, thereby preventing the disease's rapid spread. A total of more than 200 countries have been infected by COVID-19, with more than 100 000 domestic confirmed cases and more than 95 000 cured cases; more than 173 million confirmed cases globally and more than 139 million fixed cases. Table 1 displays statistics on the nationwide outbreak.

Deep learning is increasingly being used in the medical profession at the moment. Convolutional neural networks are very successful in solving challenges related to medical image processing and computer vision. Numerous layers comprise the convolutional neural network—automatic feature extraction from picture data. The technique has been used to a variety of medical pictures, including breast lesions segmentation, brain and skin lesions segmentation, and lung nodule segmentation; on the other hand, deep learning and computer vision are utilized to diagnosis illnesses considerably more correctly than radiologists. As a result, incorporating deep learning technology into radiology enables more precise diagnosis. Convolutional neural networks can considerably increase the speed and accuracy of CT image identification of new coronary pneumonia by recognizing images with critical traits in order to authenticate covid-19 test. As is well known, deep learning techniques require a huge number of sample data, but convolutional neural networks require a big amount of data and computational resources yet produce superior results on large data sets. As a result, given the restricted size of the public dataset, it is required to enrich it using a variety of data augmentation techniques. Deep learning is currently being applied quite extensively in the health world. Convolutional neural networks have turned out to be exceptionally powerful at fixing things in medicinal computer vision and image processing. The author (Yang et al., 2021) conducted a thorough assessment of relevant research on existing image enhancement techniques and presented typical study findings for each category of augmentation research; the author (Wu et al., 2020) extended the usage of CXR pictures with sparse labeling. This document describes the different issues that individuals and health professionals are encountering as a result of COVID-19. Several methods for controlling the effect of COVID-19 employing Internet of things are explored in this study (Ajaz et al., 2022).The distribution of training data for supervised learning was investigated, and it was shown that performance may be considerably improved by integrating basic weakly labeled augmentation training data into the original dataset; Author proposed incorporating traditional data augmentation techniques such as flipping, rotation, and elastic deformation, as well as random cropping and synthetic data generation methods based on generative adversarial networks; Author used GAN to generate multiple X-ray images and selected three deep transfer models with the highest possible accuracy for research. X-ray imaging revealed the infection (Soni et al., 2022). GANs (Generative Adversarial Networks) are convolutional infrastructure that can generate images with conceptual annotations that can be utilized to enrich data.Deep learning methods are frequently employed in medical imaging because they can automatically or via pre-trained networks retrieve characteristics. Author (Xu et al., 2022) classified liver CT pictures using three support vector machine approaches, neural network, and random forest, and obtained favorable results; Author (Churi et al., 2021) classified blood vessels in chest CT images using three-dimensional CNN. Classified as arteries and veins, and when compared to a random forest classifier, the suggested technique achieved a better classification accuracy; Author (Hi ş am and Hi ş am, 2021; Patil & Golellu, 2021) increased classification accuracy using an Adaptive Neuro-Fuzzy Inference System (ANFIS) based on particle swarm optimization (Wang et al., 2020). Compared seven deep learning models utilizing the COVIDX-Net method, which obtained up to 90% accuracy using VGG19 and DenseNet201. However, this study is limited by its tiny sample size. Additionally, Author (Yan et al., 2021) employed ResNet50 and support vector machine (SVM) classification to diagnose COVID-19 utilizing X-ray pictures, with a total of 50 chest X-ray images used in the experiment. The author employed transfer learning-based approaches and deep architectures such as ResNet50, Inception v3, and others to develop deep convolutional neural networks for the purpose of automatically detecting COVID-19 in X-ray pictures. Computer-aided diagnostic system is a machine approach that assists clients in making smart choice. Due to the small size of patients, the depth of the network model is excessive. The chance of being over fit increases. On the basis of the foregoing, this study proposes to employ CGAN technology to augment the restricted data set, integrate the residual block into the U-Net network, and combine multi-layer perception in order to construct new network architecture for COVID-19 detection using CT images. −19. Given the scarcity of COVID-19 CT datasets, it is proposed that conditional generative adversarial networks be used to augment data in order to obtain CT datasets with more samples and therefore lower the danger of overfitting. A BIN residual block-based technique is also proposed in this paper. For picture segmentation, the enhanced U-Net network is utilized, followed by multi-layer perception for classification prediction. When compared to network models such as AlexNet and GoogleNet, the suggested BUF-Net network model is shown to have the best performance, with a 93 percent accuracy rate. In this research the important function of CT images in diagnosing COVID-19 can be more easily illustrated by using Grad-CAM technology to depict the system's output.

Table 1
Global epidemic data as of June 8, 2021

Area	The cumulative number of confirmed cases	Cumulative death toll	Case fatality rate/%
China	11,4707	5 132	4.47
America	33,377,632	597,946	1.79
India	28,909,975	349,186	1.2
Brazil	16,947,062	473,495	2.79
Russia	5,135,866	124,117	2.41
U.K	4,522,476	152,068	3.36
Italy	4,232,428	126,523	2.98
Germany	3,717,890	89,825	2.41

When compared to the assessment indicators of a variety of network models, the conditional generative adversarial network proves to be a great tool for data augmentation. Furthermore, with a classification accuracy of 93.1 percent, the improved model proposed in this study performs the best overall.

Organization: The study is organised as follows section 1 is introduction of the problem statement followed by section 2 which is about Material (Data set). Section 3 elucidates about the Methods, followed by section 4 that states the results and the final section is conclusion.

2. Material

2.1. Dataset

The experiment employed the publicly available COVID-19 CT dataset (https://github.com/UCSD-AI4H/COVID-CT), which comprises 349 COVID-19 pictures and 397 non-COVID-19 images from 216 patients. Nineteen photos supplement the dataset with additional samples and reduce over-fitting using a conditional generative adversarial network. Table 2 illustrates the data distribution. An example of a CT image dataset is provided in Fig. 1, with COVID-19 CT pictures on the left and non-COVID-19 CT images on the right. Classification and Segmentation system are employed for accomplishing COVID-19 CT chest assessments in real - time basis and with justifications.

2.2. Data preprocessing

The preprocessing operations performed in the experiments included:

(a) Thresholding the CT image to remove very bright pixels;
(b) rotating the CT image by 15°, flipping it horizontally (to handle pneumonia symptoms on both sides of the chest), Width offset, height offset, scaling and random cropping (to obtain deeper pixel relationships), etc.;
(c) Standardize CT images to make pixel values uniform in the (0, 1) range to reduce computational complexity;
(d) Median filtering of CT images to remove noise and preserve edges;
(e) Data augmentation of the dataset through conditional generative adversarial networks to expand the dataset and reduce the risk of over fitting. Fig. 2 shows the effect of enhancing the data using the data augmentation method.

3. Methods

3.1. Data augmentation methods

3.1.1. Generative adversarial networks

GAN is implemented to generate multiple X-ray images and selected three deep transfer models with the highest possible accuracy for research. X-ray imaging revealed the infection. GANs (Generative Adversarial Networks) are convolutional infrastructure that can generate images with conceptual annotations that can be utilized to enrich data Different methods for controlling the effect of COVID-19 employing internet of things technology are proposed in this research (Mehbodniya et al., 2021).

Generative adversarial network GAN (generative adversarial network), a network model that first appeared in 2014, is a deep learning model invented by author (Hu et al., 2020). The generator (Generator) and the discriminator (Discriminator) two parts make up the GAN. Extensive experiments have demonstrated that GANs can effectively deal with the problem of too few samples in datasets. For example, author (Gomathi et al., 2020) used GAN to generate synthetic medical images to improve the accuracy of classification performance; author (Guo et al., 2021) proposed a GAN-based architecture for limited training data scenarios, and the result was a model capable of Diversity is achieved in the generated samples. Author (Niu et al., 2021) also used GAN as a data augmentation method to show that it can improve performance in tumor segmentation. The construction of GAN is shown in Fig. 3.

The GAN loss function V (D, G) consists of the discriminator maximizing the loss function maxD and the generator minimizing the loss function minG:

$$\min_{c}\max_{d} V(d,g) = E_{pdata(x)}\left[\log\left(D\left(\frac{x}{y}\right)\right)\right] + E_{p(z)}\left[\log\left(1 - D\left(g\left(\frac{z}{y}\right)\right)\right)\right]$$

In the formula, x denotes the actual image and z denotes the noise image; D(x) denotes the discriminator's judgment value for the

Table 2
Dataset distribution of CT images.

Dataset	Train set		Validation set		Test set	
	COVID-19	NonCOVID-19	COVID-19	NonCOVID-19	COVID-19	NonCOVID-19
COVID19	244	278	71	80	34	39
COVID19+	1466	1667	419	476	209	239

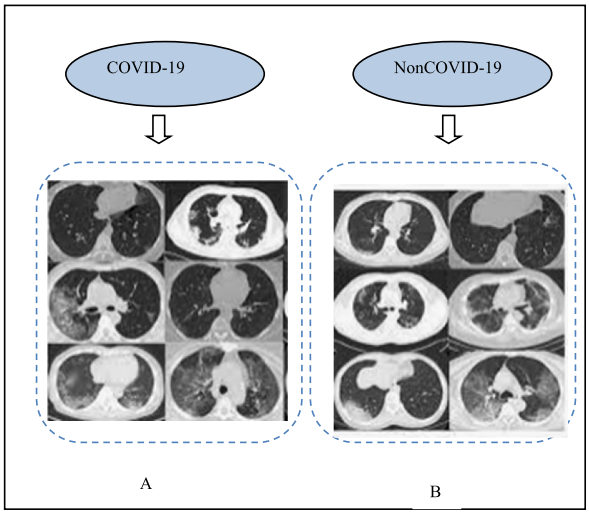

Fig. 1. Example of CT image dataset.

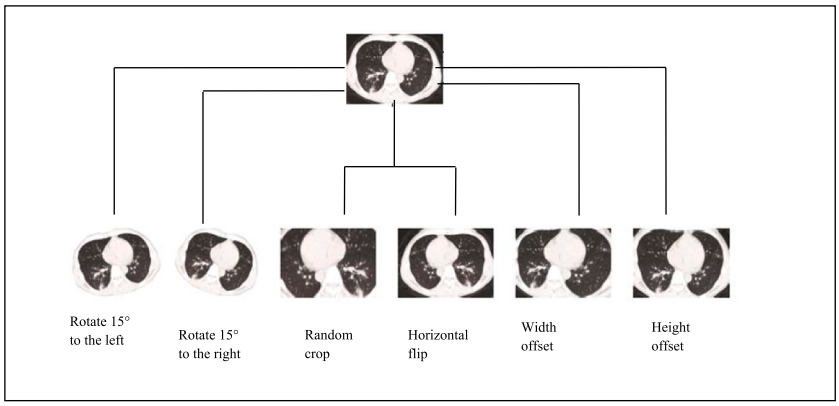

Fig. 2. Example of the data enhancement effect.

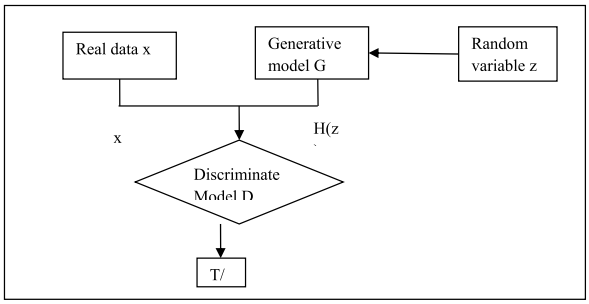

Fig. 3. Generative adversarial network structures.

exact image; D (G(z)) denotes the discriminator's judgment value for the generated image G(z); Pdata (x) denotes the distribution of the actual image; Pz(z) denotes the distribution of the noise image. ExPdata(x) denotes the expectation that x is sampled from the real image's distribution; EzPz(z) denotes the expectation that z is sampled from the noise image's distribution.

The generator accepts x as an input model, and the convolution operation on x can extract information about the image's features. The generated z is consistent with the original image distribution image G. (z). The smaller the loss function of the generator V(G), the more similar G(z) is to x. The discriminator G(z) will simultaneously accept x as input and will need to determine whether G(z) is consistent with x. V(D) of the discriminator's loss function is in the range [0, 1]. When V(D) equals 1, the generated picture G(z) is

compatible with the original image x; when V(D) equals 0, G(z) is completely discordant with x. The greater V(D), the closer G(z) is to x. G(z) is made as identical to x as possible by the discriminator, resulting in D. (x). The generator and discriminator play a game until the generator generates G(z) that is endlessly close to x

3.1.2. Conditional generative adversarial networks

The CGAN is made up of two distinct types of networks, the generator network and the discriminator network, the structure of which is seen in Fig. 4. The conventional adversarial generative network model can only learn one class of input at a time. Because it must be comprehended layer by layer for sample sets containing numerous courses, the model bears the flaw of inefficiency. In comparison, the CGAN model adds the same requirements to the generator, and GAN can create multi-class data in the discriminator. The generating network utilized in this article is composed of six transposed convolutional layers, five ReLU layers, five batch normalization layers, and a Tanh layer at the output. Six convolutional layers, five leaky ReLUs, and four batch normalizations comprise the discriminator network. Table 3 illustrates the CGAN structure used in this paper. In comparison to conventional GAN, CGAN alters the total loss function, including the formula (2)

$$min_H min_E W(E,H) = min_H min_E (F_{x-Qdata}(In\ E(x|Y)) + F_{Z-QZ(Z)}(In(1-E(x|Y)))) \tag{2}$$

Due to the limited publicly available COVID-19 CT image dataset; this paper uses a CGAN network to overcome the over fitting problem caused by the limited number of CT images in the COVID-19 dataset, which increases the dataset images to 6 times the original sample. Data augmentation helps achieve better segmentation accuracy and performance matrix, and the completed performance measures are discussed in the experimental results section.

3.2. Improved U-Net network

3.2.1. U-Net network

U-Net is a fully connected image segmentation network based on CNN that is commonly used in medical picture segmentation. The U-Net model is a nearly symmetrical U-shaped structure. The left side of U represents a procedure known as down sampling, while the right side represents a method known as up sampling. Fig. 5 illustrates its structure. Numerous investigations have demonstrated that U-Net is an excellent candidate for semantic segmentation of medical images. Author (Rohmah & Bustamam, 2020) combined self-supervised learning and supervised segmentation to accomplish hybrid led learning for breast ultrasound images using an enhanced U-Net algorithm. To increase image segmentation accuracy, the author used the Resnet module with convolutional attention in the encoding part of the U-Net network to organize the output features and thus improve blood vessel segmentation accuracy (Pratiwi et al., 2021). Accuracy; developed a fusion neural network for ultrasound foetal head edge identification using the U-Net network and the last layer of U-Net++ features. The encoding portion is comparable to a compression procedure in that it obtains deeper features (i.e. low resolution and low-resolution features). The decoding section returns the deeply encoded elements to the final output image at its original size (Enshaei et al., 2021, pp. 1–6).

The construction of the U-Net network is primarily made of convolutional layers, maximum pooling layers, DE convolutional layers, and a ReLU activation function. Given the fuzzy boundaries and complicated gradients present in medical images, the underlying information is critical for effective segmentation. As a result, the U-Net network model incorporates both high- and shallow-level semantic and geographical information.

3.2.2. Improved U-Net network

3.2.2.1. Residual block. To solve the problem that the more profound the deep neural network is, the higher the error rate and the longer the training time will be. In 2016, author proposed the residual network (ResNet) model in the ImageNet image recognition competition adding the input result directly to the bottom layer by adding a direct channel to the network. The idea is shown in formula (3):

$$D(x) = x + G(x) \tag{3}$$

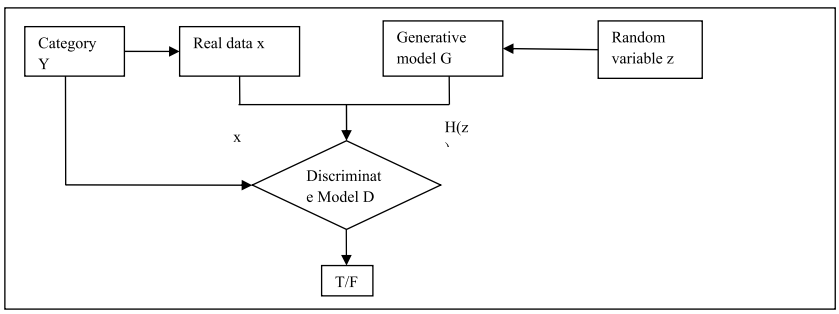

Fig. 4. Conditional generative adversarial network structures.

Table 3
Conditional generative adversarial network the system used in this article.

Generator Network	Discriminator Network
Enter	Enter
Transpose Convolution 1	Convolution 1
Batch Normalization 1	Leaky ReLU1
ReLU1	Convolution 2
Batch Normalization 2	Batch Normalization 1
Transpose Convolution 2	Leaky ReLU2
ReLU2	Convolution 3
Transpose Convolution 3	Batch Normalization 2
Batch Normalization 3	Leaky ReLU3
ReLU3	Convolution 4
Transpose Convolution 4	Batch Normalization 3
ReLU4	Leaky ReLU4
Transpose Convolution 5	Convolution 5
Batch Normalization 4	Batch Normalization 4
Batch Normalization 5	Leaky ReLU5
ReLU5	Convolution 6
Transpose Convolution 6	
Tanh	

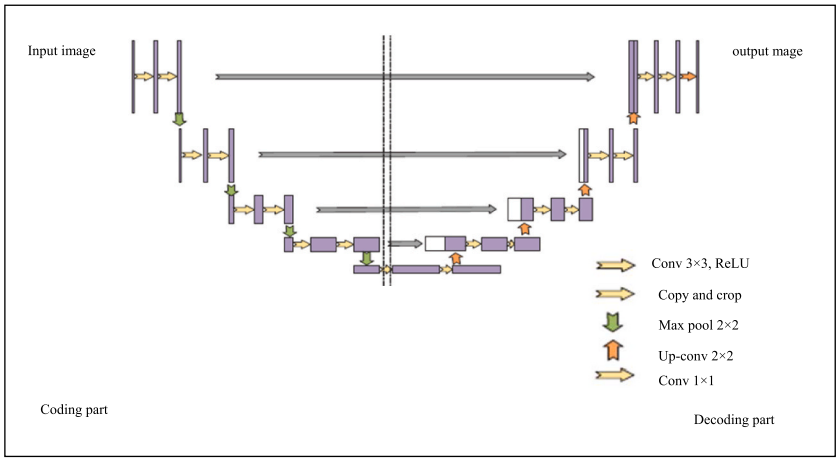

Fig. 5. U-Net network structures.

Among them, x is the input, G(x) is the output of the hidden layer, and D(x) is the underlying map. The structure of the residual block is shown in Fig. 6.

3.2.2.2. Improved U-Net network. The residual block in the residual network is integrated into U-Net, which largely avoids the occurrence of over fitting and can effectively reduce the gradient disappearance problem caused by the deepening of the network structure, thereby improving the segmentation performance of the model. . This paper adopts a modified BIN residual block for batch normalization after each convolution. As a result, the BN layer can improve the generalization ability of the network and accelerate the training of the network model, as shown in formula (4):

$$CN(x) = \gamma \frac{x - w(x)}{\sigma(x)} + \beta \tag{4}$$

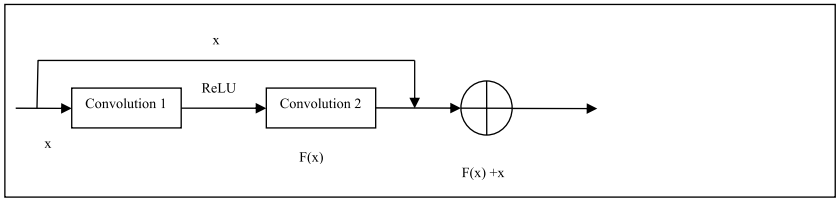

Fig. 6. Residual block structure.

where $x \in \mathbb{R}^{M \times C \times H \times W}$ is the input of the CN layer, $\gamma \in \mathbb{R}^{C}$ and $\beta \in \mathbb{R}^{C}$ are the mapping parameters learned from the data, and $u(x) \in \mathbb{R}^{C}$ and $\sigma(x) \in \mathbb{R}^{C}$ are the input mean and standard deviation.

$$\mu_d(x) = \frac{1}{MHW}\sum_{m=1}^{M}\sum_{h=1}^{H}\sum_{w=1}^{W} x_{mchw} \tag{5}$$

$$\sigma_d(x) = \sqrt{\frac{1}{MHW}\sum_{m=1}^{M}\sum_{h=1}^{H}\sum_{w=1}^{W}\left(x_{mchw} - \mu_d(x)\right)^2 + \varepsilon} \tag{6}$$

Author proposed that the JN layer (instance-normalization) model faster train. The calculation formula of the JN layer is formula (7)~(9):

$$JN(x) = \gamma\frac{x - w(x)}{\sigma(x)} + \beta \tag{7}$$

$$\mu_d(x) = \frac{1}{HW}\sum_{m=1}^{M}\sum_{w=1}^{W} x_{mchw} \tag{8}$$

$$\sigma_d(x) = \sqrt{\frac{1}{MHW}\sum_{m=1}^{M}\sum_{w=1}^{W}\left(x_{mchw} - \mu_d(x)\right)^2 + \varepsilon} \tag{9}$$

Author proved that adding a CN layer can significantly accelerate the convergence of the model by explaining the specific operation process of CN. As shown in formulas (10) and (11):

$$\hat{x_i} = \frac{x_i - \mu_C}{\sqrt{\sigma\, C^2 + \varepsilon}} \tag{10}$$

$$y_i = \gamma\, \hat{x_i} + \beta \tag{11}$$

Where μC and σ2C represent the mean and variance of the dataset, respectively, the normalized data $\hat{x_i}$ is input to the network, and there is no need to adjust the network learning to adapt to the change of data distribution in the subsequent process.

The CN layer and the JN layer with the same number of channels are simultaneously introduced to the residual block's two-layer network in this research. All CN-based residual blocks in the original model are replaced by the BIN-based residual block, which simultaneously satisfies the JN layer. And the characteristics of the CN layer will increase the model's convergence speed, as the model will no longer rely on the delicate parameter initialization process; secondly, a more significant learning rate can be chosen to avoid gradient explosion during the back propagation process; additionally, it will reduce the frequency of use of the dropout layer and improve the model's generalisation ability to a certain extent. Fig. 7 illustrates the comparison of the two leftover block structures. The residual block structure based on the CN layer is depicted in Fig. 7(a), whereas the residual block structure based on the BIN layer is

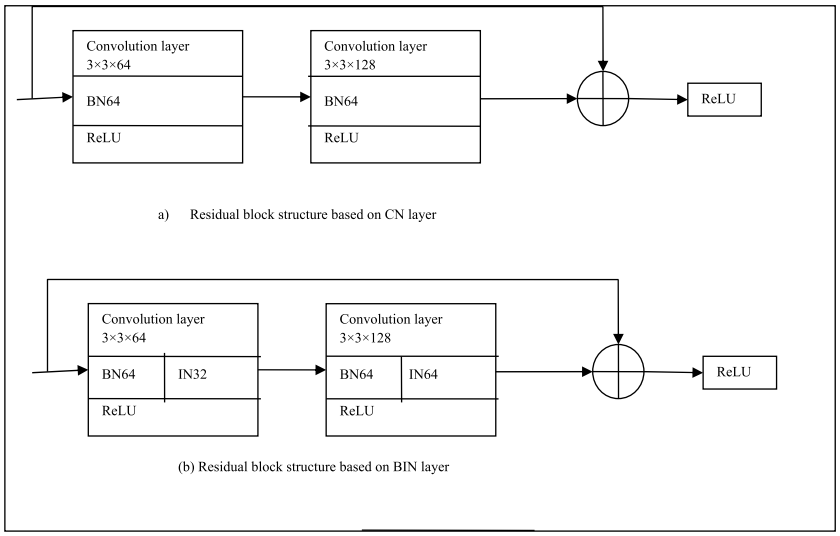

Fig. 7. Comparison of residual block structure.

depicted in Fig. 7(b). The BIN layer is composed of a CN layer with 32 channels and a JN layer with 32 tracks, followed by the addition of the CN layer. Additionally, JN layers can accelerate the loss's convergence while preserving the semantic information associated with the learned features.

The activation function used by the improved U-Net network is the sigmoid function, and the loss function Loss is based on the Dice_coef coefficient, as shown in formulas (12) and (13):

$$Dice_{Coef} = \frac{2*(Y \cap X) + smooth}{|Y| + |X| + \ smooth} \tag{12}$$

$$Loss = \ - \ Dice_{Coef} \tag{13}$$

3.3. Model of this paper

The algorithm used in this paper mainly includes three steps:

1) Preprocessing. First, basic preprocessing operations are performed on the collected COVID-19 CT dataset, especially flipping, rotating, offsetting, scaling, etc. The dataset is then augmented with conditional generative adversarial networks to increase the number of samples.
2) Model creation. This article presents a model that is a combination of segmentation and classification. To be more precise, lung lesions were obtained using a segmentation model and then classified to determine whether each lesion was a COVID-19 symptom. Segmentation is represented mathematically using an upgraded U-Net network. By alternating between convolutions and pooling procedures, the encoder component lowers the spatial dimension. Convolutional operations are utilized to substitute totally connected layers in the encoding and decoding layers, which can be more efficient—achieves good hierarchical characteristic extraction. Two 33 convolutions, a 33 BIN residual block, and a 22 pooling operation are used. Convolution is used to perform a pre-processing method on the image. The first layer of convolution reduces the number of channels and sends the data to the second layer of convolution for processing in order to recover the media of the feature map. The residual block mixes the input features with the result of the two-layer convolution, significantly reducing the vanishing gradient. Pooling is used to reduce parameters and avoid over fitting. The decoder part is symmetrical to the encoder section in order to recover spatial dimension and detail lost during the pooling phase on the target. It is composed of two 33-convolutional layers, a 33-BIN residual block, and finally a single convolutional layer for classification. The deconvolution operation can reduce the number of channels in half while doubling the resolution of the feature map. The improved U-Net network generates a 32321024 tensor, which is subsequently flattened for classification purposes. The multi-layer perceptron (MLP) is activated by ReLU and is made of two thick layers of 128 and 64 neurons, respectively. Finally, the activation function is a sigmoid; for image classification, a dense layer with one neuron is utilized. The wrong type was determined by averaging 1.79 s for CT image admission into the network.
3) Performance evaluation: evaluate the pros and cons of the proposed algorithm through a series of evaluation indicators. And use Grad-CAM technology.

3.4. Experimental design

3.4.1. Experimental environment

This experiment chooses to implement on the Windows10 operating system. It uses the Kersaf library on Tensor flow backend to develop and run a deep learning network for experimental verification, supporting CUDA10.0 and the CUDNN8 acceleration package. The environment for the experiment running is python3.7, i5-8265U2.30 GHz CPU, and memory is 8 GB.

3.4.2. Experimental setup

The COVID-19 CT images were retrieved and categorized in the experiment using an upgraded U-Net network model in conjunction with a multilayer perceptron. During the training process, the model set the initial learning rate to 0.001 and the momentum to 0.9. Additionally, the early stopping approach is applied. To avoid the network over fitting, the training can be halted in advance when the outcome consistently reaches a predefined, accurate value. The model is trained for 100 epochs with a setting of 40. Then, choose a Stochastic Gradient Descent (SGD) optimizer whose learning rate decays at a rate equal to the initial learning rate divided by the number of training epochs. The following hyperparameters of the model are then optimized using a stochastic grid search method: (1) momentum; and (2) the SGD optimizer's initial learning rate.

3.4.3. Evaluation indicators

Five separate evaluation indicators are employed to validate the method suggested in this work for detecting new coronary pneumonia using CT images: Accuracy, Precision, Sensitivity, F1-score, and Specificity. The right rate quantifies the proportion of correctly identified samples across all samples. As defined in formula (14); precision as defined in formula (15), which relates to the ratio of correctly identified samples to the total number of correctly identified pieces; The sensitivity, or recall rate, is used to determine how many positive examples are accurate discrimination, as shown in equation (16); both sensitivity and precision can be calculated from the confusion matrix, and the F1-score is a comprehensive evaluation factor for both accuracy and sensitivity, as shown in equation (17); specificity is expressed in all of these equations. The proportion of paired parts in negative examples of, as

stated in Equation (18); AUC denotes the "area beneath the receiver operating characteristic curve," and is less susceptible to class imbalance than ACC.

$$\text{Accuracy} = \frac{\text{UP} + \text{UN}}{\text{Up} + \text{Un} + \text{Gp} + \text{GN}} \tag{14}$$

$$\text{Precision} = \frac{\text{UP}}{\text{UP} + \text{GP}} \tag{15}$$

$$\text{Sensitivity} = \frac{\text{UP}}{\text{UP} + \text{GP}} \tag{16}$$

$$\text{G1} - \text{score} = 2 \times \frac{\text{Precision} * \text{Sensitivity}}{\text{Precision} + \text{Sensitivity}} \tag{17}$$

$$\text{Specificity} = \frac{\text{TP}}{\text{GP} + \text{UN}} \tag{18}$$

Among them, UP denotes the number of successfully categorized positive examples; The number of positive measures that are appropriately identified as bad examples is represented by the UN; GP denotes the number of models categorized incorrectly as positive examples, also referred to as the false positive rate; GN denotes the number of mistakenly classified positive measures as negative examples Quantity, alternatively referred to as the false-negative rate.

4. Results

To validate the model's performance, a fivefold cross-validation approach was used. The training data were separated randomly into five sections, four of which were designated as the training set and the remaining four as the validation set. This procedure is done five times in order to train and test the suggested method described in this research. To demonstrate the success of the model (BUF-Net) given in this research, the method is compared to numerous others proposed in the literature. The performance indicators (sensitivity, accuracy, and G1 value) for each model and sensitivity are listed in Table 4. As can be shown, the model provided in this study has an accuracy and precision of 97.1 percent and 93.1 percent, respectively, and a specificity value that is lower than that of previous models. Additionally, the majority of other models do not depict the categorization findings using Grad-CAM technology.

A confusion matrix is also a performance measure that provides a deeper insight into the test accuracy achieved by the proposed model. Table 5 compares the confusion matrix of the original dataset A and dataset B after data enhancement. The results show that after the CGAN data enhancement, the proposed model is adequate for most.

All sub-samples were correctly classified, achieving an accuracy of 97.1%. The convergence comparison between the improved convolution neural network and the original U-Net network combined with the multi-layer perceptron model. It can be seen that the model has better convergence after replacing the original residual block with the BIN residual block, and compared with before adding the BIN residual block, the convergence speed is greatly improved in the 4th to 18th rounds, and after iterating to the 26th round, the convergence speed remains unchanged. Table 6 and Fig. 8 shows the performance comparison between the models proposed in this paper and other classical algorithm in the original and the data-enhanced data sets. The results show that AlexNet has the highest sensitivity in scenario 1, at 87.9%, which refers to the correct classification of the capacity of COVID-19 CT. While GoogleNet has better specificity, the value increases slightly after data enhancement. Before data enhancement, the accuracy of VGGNet16 has been dramatically improved, from 75% to 90%. Both VGG16 and GoogleNet have 16 layers and contain many parameters. The model proposed in this paper has apparent improvements in the four indicators of accuracy, precision, sensitivity and F1 index.

The experimental results indicate that the BUF-Net model outperforms other techniques in general. After data augmentation, the commission's accuracy increased dramatically, reaching 93%, which is 9% higher than before CGAN data enhancement. As a result, conditional generative adversarial networks are a useful technique for data augmentation. The ROC curve for the algorithm described in this paper is shown in Fig. 9 and the AUC value for BUF-Net is 0.932. To avoid over fitting, the rounds are adjusted to 40 using the early stopping strategy technique. As illustrated in the picture, the accuracy and loss value reach an equilibrium point where the loss remains constant between 1.3 and roughly 0.13.

Table 4
Comparison of BUF-Net algorithm with other algorithms.

Paper	Model	Sen	Acc	Spe	Pre
[28]	Attention ResNet34+Dual Sampling	86.9	87.5	90.1	
[29]	AFS-DF	93.1	91.7	89.9	
[30]	DarkCovidNet	85.3	87		89.9
[31]	COVID-Net	91	93.3		98.9
[32]	GLSZM-LSTM	97.5	98.7	99.6	99.6
ours	BUF-Net	87.6	93.1	77.3	97.1

Table 5
Confusion matrix.

	Covid 19	Non Covid 19			Covid 19	Non Covid 19	
Covid 19	293	56	846%.	**Covid 19**	1834	260	87.6%
	39.3%	7.5%	6%		41%	5.8%	12.4%
Non Covid 19	64	333	83.9%	**Non Covid 19**	54	2328	97.7%
	8.6%	46.3%	16.1%		1.2%	52%	2.3%
	82.1%	85.6%	83.9%		97.1%	90%	93%
	17.9%	14.3%	16.1%		2.9%	10%	7%
	(a) Covid 19				**(b) Covid 19 +**		

Table 6
Performance comparison.

Serial	AlexNet	VGGNet16	GoogleNet	Model
Sensitivity	0.9	0.6	0.65	0.85
Precision	0.5	0.7	0.6	0.8
F1	0.6	0.8	0.5	0.85
score	0.7	0.5	0.55	0.8
Accuracy	0.8	0.4	0.4	0.75
Specificity	0.5	0.6	0.45	0.8

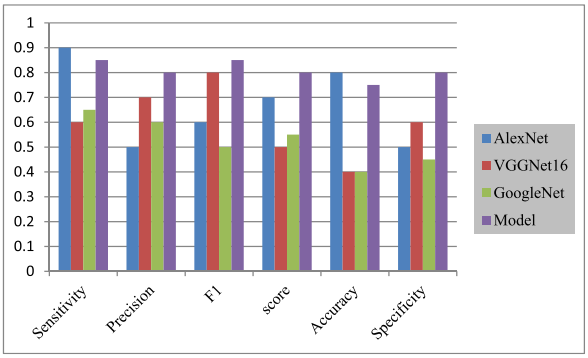

Fig. 8. Performance comparison.

The output results are visualized using a gradient-weighted activation map (Grad-CAM) to generate classification zones that facilitate visualizing the infection distribution in lung nodules on CT images. Grad-CAM is a visualization technique for gradients. The CAM technique is limited to a specific design in which convolutional layers are coupled via an average pooling layer to a fully connected layer. The gradient for a particular class is derived using the features recovered by the trained model's deepest convolutional layer and fed into a global average pooling layer to obtain the decision's real weights. This produces a two-dimensional heat map, which is a weighted mixture of feature maps used to classify images. The results of the visualization are depicted in Fig. 10. The red and light blue patches indicate regions that have been activated by the deep neural network, whilst the dark purple background indicates inactive regions. Grad-CAM results indicate that the proposed model is effective for COVID-19 CT detection.

5. Conclusions

This paper demonstrates that when compared to standard methods, deep learning methods can increase diagnostic efficiency and treatment quality. While the paper's proposed better network topology for segmentation and joint classification can improve accuracy, it still has certain drawbacks. The data set targeted in this investigation has a limited sample size, and the results are prone to over fitting. As a result, additional work is required. With the application of deep models to larger datasets, it is also required to investigate further data augmentation techniques in order to validate the performance of the research methodologies provided in this study.The purpose of this paper is to propose a novel method for augmenting the dataset using conditional generative adversarial networks in order to reduce the risk of over fitting due to the small sample size of the original dataset; additionally, the enhanced CT image dataset is input into an improved U-Net network for medical segmentation, which is combined with multilayer perceptron's for binary classification. The u-net is a convolutionary neural topology for image analysis that seems to be fast and efficient way. Comparing the conditional generative adversarial network to the evaluation indicators of numerous different network models demonstrates that it is an excellent tool for data augmentation. Additionally, the modified model described in this research performs the best overall, with a classification accuracy of 93.1 percent. Finally, the output results are visualized using Grad-CAM technology, emphasizing the crucial

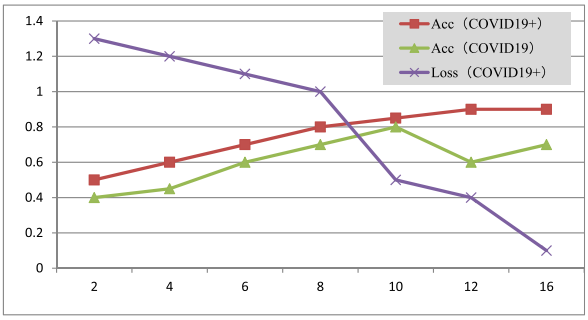

Fig. 9. ROC curve and model training curve of BUF-Net.

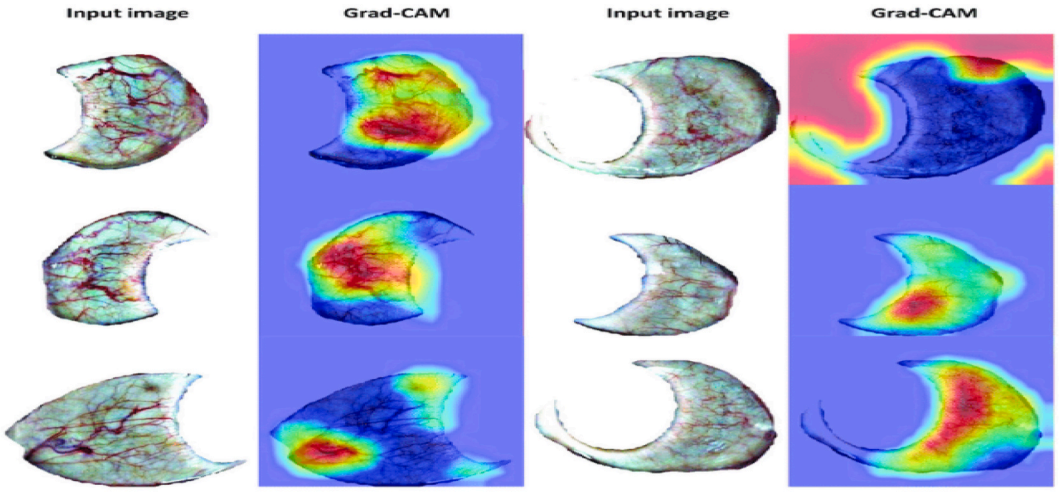

Fig. 10. Grad-CAM visualization results.

importance of CT pictures in detecting COVID-19 and the efficacy of the BUF-Net method described in this research for predicting COVID-19 CT images.Effectiveness of BUF-Net method in contrast to COVIDX-Net model is supplementary.Therefore applying deep learning using the proposed techniques suggested by the above study in medical imaging can help radiologists achieve more effective diagnoses that is the main objective of the research with the future trends to be employing the same technique to detect other fatal criticality other than viral diseases.

Credit author statement

Mukesh Soni: Methodology, validation, Supervision **Ajay Kumar Singh**: Conceptualization, Resources **K. Suresh Babu:** Writing original draft, Data curation **Sumit Kumar:** Software, Validation **Akhilesh Kumar:** Investigation, Formal analysis **Shweta Singh:** Writing-Reviewing & Editing.

Declaration of competing interest

The authors declare that they have no known competing financial interests or personal relationships that could have appeared to influence the work reported in this paper.

References

Ajaz, F., Naseem, M., Sharma, S., Shabaz, M., & Dhiman, G. (2022). COVID-19: Challenges and its technological solutions using IoT. *Current Medical Imaging Reviews, 18*(2), 113–123. https://doi.org/10.2174/1573405617666210215143503

Churi, P., Mistry, K., Asad, M. M., Dhiman, G., Soni, M., & Kose, U. (2021). "Online learning in COVID-19 pandemic: An empirical study of Indian and Turkish higher education institutions". *World Journal of Engineering*. https://doi.org/10.1108/WJE-12-2020-0631. ahead-of-print No. ahead-of-print.

Enshaei, N., et al. (2021). *An ensemble learning framework for multi-class covid-19 lesion segmentation from chest ct images*. 2021 IEEE International Conference on Autonomous Systems (ICAS). https://doi.org/10.1109/ICAS49788.2021.9551169

Gomathi, S., Kohli, R., Soni, M., Dhiman, G., & Nair, R. (2020). Pattern analysis: Predicting COVID-19 pandemic in India using AutoML. *World Journal of Engineering*. https://doi.org/10.1108/WJE-09-2020-0450. ahead-of-print No. ahead-of-print.

Guo, G., Liu, Z., Zhao, S., Guo, L., & Liu, T. (May 2021). "Eliminating indefiniteness of clinical spectrum for better screening COVID-19,". *IEEE Journal of Biomedical and Health Informatics, 25*(5), 1347–1357. https://doi.org/10.1109/JBHI.2021.3060035

Hişam, D., & Hişam, E. (2021). Deep learning models for classifying cancer and COVID-19 lung diseases. *2021 Innovations in Intelligent Systems and Applications Conference (ASYU)*, 1–4. https://doi.org/10.1109/ASYU52992.2021.9598993

Hu, S., et al. (2020). Weakly supervised deep learning for COVID-19 infection detection and classification from CT images. *IEEE Access, 8*, 118869–118883. https://doi.org/10.1109/ACCESS.2020.3005510

Jiang, Y., Chen, H., Loew, M., & Ko, H. (Feb. 2021). COVID-19 CT image synthesis with a conditional generative adversarial network. *IEEE Journal of Biomedical and Health Informatics, 25*(2), 441–452. https://doi.org/10.1109/JBHI.2020.3042523

Mehbodniya, A., Alam, I., Pande, S., Neware, R., Rane, K. P., Shabaz, M., & Madhavan, M. V. (2021). Financial fraud detection in healthcare using machine learning and deep learning techniques. *Security and Communication Networks, 2021*, 1–8. https://doi.org/10.1155/2021/9293877

Niu, S., Liu, M., Liu, Y., Wang, J., & Song, H. (2021). "Distant domain transfer learning for medical imaging,". *IEEE Journal of Biomedical and Health Informatics, 25*(10), 3784–3793, Oct. https://doi.org/10.1109/JBHI.2021.3051470

Patil, S., & Golellu, A. (2021). Classification of COVID-19 CT images using transfer learning models. *2021 International Conference on Emerging Smart Computing and Informatics (ESCI)*, 116–119. https://doi.org/10.1109/ESCI50559.2021.9396773

Pratiwi, N. G., Nabila, Y., Fiqraini, R., & Setiawan, A. W. (2021). Effect of CT-scan image resizing, enhancement and normalization on accuracy of covid-19 detection. *2021 International Seminar on Intelligent Technology and Its Applications (ISITIA)*, 17–22. https://doi.org/10.1109/ISITIA52817.2021.9502217

Rohmah, L. N., & Bustamam, A. (2020). Improved classification of coronavirus disease (COVID-19) based on combination of texture features using CT scan and X-ray images. *2020 3rd International Conference on Information and Communications Technology (ICOIACT)*, 105–109. https://doi.org/10.1109/ICOIACT50329.2020.9332123

Soni, M., Gomathi, S., Kumar, P., Churi, P. P., Mohammed, M. A., & Salman, A. O. (2022). Hybridizing convolutional neural network for classification of lung diseases. *International Journal of Swarm Intelligence Research, 13*(2), 1–15. https://doi.org/10.4018/IJSIR.287544

Wang, J., et al. (2020). Prior-attention residual learning for more discriminative COVID-19 screening in CT images. *IEEE Transactions on Medical Imaging, 39*(8), 2572–2583, Aug. https://doi.org/10.1109/TMI.2020.2994908

Wu, X., Wang, Z., & Hu, S. (2020). Recognizing COVID-19 positive: Through CT images. *2020 Chinese Automation Congress (CAC)*, 4572–4577. https://doi.org/10.1109/CAC51589.2020.9326470

Xu, G.-X., et al. (Jan. 2022). "Cross-Site severity assessment of COVID-19 from CT images via domain adaptation,". *IEEE Transactions on Medical Imaging, 41*(1), 88–102. https://doi.org/10.1109/TMI.2021.3104474

Yan, Q., et al. (1 March 2021). COVID-19 chest CT image segmentation network by multi-scale fusion and enhancement operations. *IEEE Transactions on Big Data, 7*(1), 13–24. https://doi.org/10.1109/TBDATA.2021.3056564

Yang, Z., Zhao, L., Wu, S., & Chen, C. Y.-C. (June 2021). Lung lesion localization of COVID-19 from chest CT image: A novel weakly supervised learning method. *IEEE Journal of Biomedical and Health Informatics, 25*(6), 1864–1872. https://doi.org/10.1109/JBHI.2021.3067465